ACS Catalysis

Research Article

pubs.acs.org/acscatalysis

Activity and Recyclability of an Iridium–EDTA Water Oxidation Catalyst Immobilized onto Rutile TiO_2

Arianna Savini,[†] Alberto Bucci,[†] Morena Nocchetti,[‡] Riccardo Vivani,[‡] Hicham Idriss,[§] and Alceo Macchioni*,[†]

[†]Department of Chemistry, Biology and Biotechnology, University of Perugia, Via Elce di Sotto 8, I-06123 Perugia, Italy

[‡]Department of Pharmaceutical Sciences, University of Perugia, Via del Liceo 1, I-06123 Perugia, Italy

[§]Corporate Research and Innovation (CRI) Centre at SABIC-KAUST, P.O. Box 4545-4700, Thuwal 23955, Saudi Arabia

Supporting Information

ABSTRACT: An iridium heterogenized catalyst for water oxidation (**1**_TiO_2) was synthesized by immobilizing the molecular precursor [Ir(HEDTA)Cl]Na (**1**) (*egg of Columbus*) onto rutile TiO_2 (*tap the egg gently on the table*). **1**_TiO_2 was evaluated as potential catalyst for water oxidation using CAN (cerium ammonium nitrate) as a sacrificial oxidant. **1**_TiO_2 exhibits TOF values between 3.5 and 17.1 min^{-1} and a TON >5000 cycles. Remarkably, the TOF of **1**_TiO_2 is almost two times higher than that of the molecular catalytic precursor **1**, under very similar experimental conditions. The reusability of **1**_TiO_2 is also remarkable. As a matter of fact, it remains active after 10 catalytic runs. Despite **1**_TiO_2 being tested under necessarily oxidative and acidic (pH 1, 0.1 M HNO_3) experimental conditions, it proved to be capable of completing more than 5000 cycles with a constant TOF of 12.8 min^{-1}, when a single aliquot of CAN was added. Some leaching of iridium from **1**_TiO_2 was observed only after the first catalytic run, leading to **1′**_TiO_2. **1**_TiO_2 and **1′**_TiO_2 were characterized by several analytical techniques. It was found that iridium atoms are uniformly dispersed on both **1**_TiO_2 and **1′**_TiO_2 samples. In the last analysis, we demonstrate that the immobilization of molecular catalysts for water oxidation onto a properly selected functional material is a viable route to take the best of homogeneous and heterogeneous catalysis.

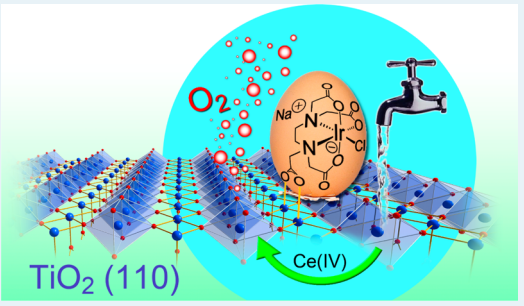

KEYWORDS: *water oxidation, immobilized catalysts, iridium complexes, rutile TiO_2, manometry, FEM-SEM, TEM, XPS*

1. INTRODUCTION

It is now evident that both the reductive generation of solar fuels, through an artificial photosynthetic process, and the production of electric energy, via a photoelectrochemical cell, strongly rely on electrons derived from water oxidation to molecular oxygen.[1−6] As a consequence, it is not surprising that considerable efforts are directed toward the development of new and better performing heterogeneous[7−10] and homogeneous[11−22] water oxidation catalysts.[23] Heterogeneous catalysts are easier to integrate in a practical apparatus and are usually more robust than homogeneous catalysts, which may transform[24] through associative processes under the harsh conditions used in catalysis. On the other hand, homogeneous catalysts can be rationally designed through the selection of the ancillary ligands, possibly guided by the knowledge of the reaction mechanism. The immobilization of a molecular catalyst onto a surface of a properly selected functional material, thus obtaining a heterogenized catalyst, has been proposed as a procedure to take the best of both worlds.[25−30] In this respect, TiO_2 is the material of choice for redox applications due to its high photocatalytic properties, low cost, stability and non-toxicity.[31−34] Nevertheless, only in a few cases have molecular catalysts for water oxidation been successfully supported onto TiO_2.[28,35−37]

Over the past few years, after the seminal papers by Bernhard[38] and Crabtree,[39] we[40−44] and others[45−54] have been involved in the synthesis of novel iridium-based molecular catalysts for water oxidation that exhibited remarkable performances. Particularly, we focused some of our attention on molecular catalysts having a pendant functionality suitable to be anchored onto a solid support.[42,43] Perhaps the most intriguing of them is [Ir(HEDTA)Cl]Na (HEDTA = monoprotonated ethylenediaminetetraacetic acid) (**1**, Scheme 1) due to the simplicity of its preparation and high solubility in water and the natural presence of a peripheral pendant −COOH functionality appropriate for immobilization on a solid support.[42] In particular, the −COOH group is suitable to interact with the dominant orientation (110) of the rutile TiO_2 surface, where the Ti···Ti distance of 3 Å allows for a stable bridging configuration, as seen by numerous studies, including scanning tunnelling microscopy,[55−57] electron-stimulated desorption ion

Received: October 15, 2014
Revised: November 22, 2014
Published: November 25, 2014

Scheme 1. Sketch of the Molecular and Heterogenized Water Oxidation Catalysts 1 and 1_TiO_2, Respectively

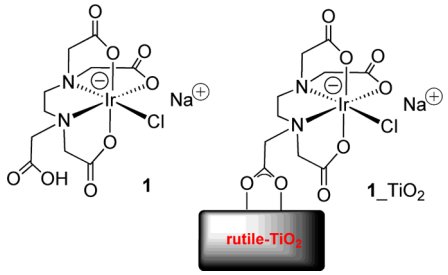

angle distribution/low energy electron diffraction,[58] IR,[59] near edge X-ray absorption fine structure,[60] X-ray photoelectron diffraction,[61,62] and density functional theory computation.[63−65] In homogeneous phase, **1** (0.5−7 μM) showed a TOF of ∼7 min^{-1} and a remarkably high TON for the catalytic oxidation of water driven by CAN (cerium ammonium nitrate).[42]

Herein, we show that **1** can be successfully immobilized onto rutile TiO_2, leading to a heterogenized catalyst (**1**_TiO_2, Scheme 1) exhibiting a higher TOF than **1** in water oxidation driven by CAN. Furthermore, **1**_TiO_2 can be reused several times with only a marginal decrease in its activity. **1**_TiO_2 and the material obtained after the first catalytic run (**1′**_TiO_2) were characterized by powder X-ray diffraction analysis (PXRD), inductively coupled plasma-optical emission spectrometry (ICP-OES), transmission electron microscopy (TEM), field emission scanning electron microscopy (FE-SEM), elemental mapping performed by X-ray spectroscopy (EDS) supported by FE-SEM, and X-ray photoelectron spectroscopy (XPS).

2. RESULTS AND DISCUSSION

1_TiO_2 was prepared by dispersing nanoparticles of rutile TiO_2 in a water solution of **1** at 25 °C (Experimental Section). **1**_TiO_2 was recovered by centrifugation and washed several times with water, 0.1 M HNO_3 water solution, acetonitrile, and dichloromethane and, finally, dried under vacuum. ICP-OES analysis (Experimental Section) indicated 0.059% w/w of iridium loading in **1**_TiO_2, corresponding to a concentration of the iridium complex of 3.1 μmol g^{-1}.

Activity of **1**_TiO_2 in water oxidation was checked by using Ce^{4+} (added as CAN) as a sacrificial oxidant, dispersing the proper amount of catalyst in acidic water (pH 1, 0.1 M HNO_3) at 25 °C.

$$4Ce^{4+} + 2H_2O \rightarrow 4Ce^{3+} + 4H^+ + O_2 \quad (1)$$

The evolved gas, according to eq 1, was quantified by differential manometry (Experimental Section).[66]

In a first series of experiments, 261, 771, and 1295 equiv of CAN with respect to the iridium were added to suspensions of ∼62 mg of **1**_TiO_2, in a total volume of 5.5 mL of acidic water (pH 1, 0.1 M HNO_3) (Table 1). Oxygen evolution was observed in all cases until complete consumption of CAN (Table 1).[67] Derived TOF values were found to increase with increasing CAN concentration from 3.5 min^{-1} up to 17.1 min^{-1} (Table 1, entries 1, 7 and 14), as often observed also for homogeneous catalysts.[31,35,36,68,69] To evaluate its reusability, **1**_TiO_2 was recovered by centrifugation and washed with acidic

Table 1. Multiple Catalytic Runs Performed with 1_TiO_2 by Adding Three Different Amounts of CAN

entry	run	C_{Ir} (μM)	C_{CAN} (mM)	C_{CAN}/C_{Ir}	$k_{obs}\cdot10^9$ (mol s^{-1})[a]	TOF (min^{-1})[b]	TON[c]	O_2 yield
1	I_{solid}	35.2[d]	**9.2**	**261**	11.2	**3.5**	46	70%
2	$I_{supernatant}$	9.5[e]	9.1	958	6.7[f]	6.9	141	59%
3	II_{solid}	24.6[g]	9.2	374	9.6	4.2	78	83%
4	$II_{supernatant}$	∼0	9.9	n.a.	∼0	n.a.	0	0%
5	III_{solid}	24.6[g]	9.3	378	8.2	3.6	77	81%
6	IV_{solid}	24.6[g]	9.3	378	5.9	2.6	72	76%
7	I_{solid}	35.0[d]	**27.0**	**771**	32.3	**10.1**	156	81%
8	$I_{supernatant}$	9.5[e]	30.0	3158	10.8[f]	13.7	622	79%
9	II_{solid}	24.5[g]	27.0	1102	16.9	7.5	228	83%
10	$II_{supernatant}$	∼0	28.6	n.a.	∼0	n.a.	0	0%
11	III_{solid}	24.5[g]	27.0	1102	13.5	6.0	214	78%
12	$III_{supernatant}$	∼0	28.6	n.a.	∼0	n.a.	0	0%
13	IV_{solid}	24.5[g]	27.0	1102	11.8	5.2	221	80%
14	I_{solid}	35.2[d]	**45.6**	**1295**	55.1	**17.1**	280	86%
15	$I_{supernatant}$	9.5[e]	50.0	5263	11.4[f]	14.3	1076	82%
16	II_{solid}	24.6[g]	45.6	1854	25.6	11.3	353	76%
17	$II_{supernatant}$	∼0	48.2	n.a.	∼0	n.a.	0	0%
18	III_{solid}	24.6[g]	45.7	1858	14.2	6.3	357	77%
19	I_{solid}	35.1[d]	45.7	1302	57.2	17.8	249	77%
20	II_{solid}	24.6[g]	45.6	1854	31.0	13.8	349	75%
21	III_{solid}	24.6[g]	45.7	1858	26.3	11.7	421	91%
22	IV_{solid}	24.6[g]	45.7	1858	20.0	8.9	412	89%
23	V_{solid}	24.6[g]	45.6	1854	15.1	6.7	407	88%

[a]From gas production (mol) vs time (s) linear trend in the initial part of the reaction. [b]From (k_{obs}/mol_{Ir})·60. [c]From total gas produced (μmol)/cat(μmol). [d]Based on a catalyst loading of 3.1 μmol g^{-1} in **1**_TiO_2 calculated from ICP-OES data. [e]Based on the fact that ICP-OES analysis indicated that 30.0% of the initial content of catalyst in **1**_TiO_2 is released into solution during the first catalytic run (I_{solid}). [f]From gas production (mol) vs time (s) in the last part of the reaction, corrected for dilution factors to better compare with values obtained in the runs with the solid. [g]Based on a catalyst loading of 2.2 μmol g^{-1} (70.0% of the initial value based on ICP-OES data).

dx.doi.org/10.1021/cs501590k | ACS Catal. 2015, 5, 264−271

water; its activity and that of the supernatant solution were tested by using the same amount of CAN of the previous experiment. Data are reported in Table 1 and Figure 1. As can

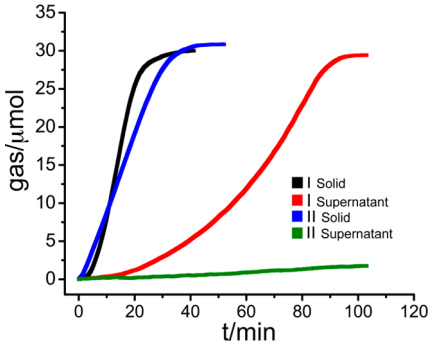

Figure 1. First two catalytic runs performed by the addition of around 150 μmol of CAN (0.5 mL) to a suspension of 62.1 mg of **1**_TiO_2 in 5.0 mL of water at pH 1 (by HNO_3). Activity of supernatant solutions was also tested by adding the same amount of CAN used in the runs with the solid.

be seen from Table 1, the recovered solid maintains most of its activity when reused. In addition, the first supernatant solution is active in water oxidation, but interestingly, the catalytic profile is rather different from that of solid materials. This is clearly shown in Figure 1, where it is possible to appreciate that **1**_TiO_2 has the typical gas evolution vs *t* trend in which, after a short induction time, there is a linear increase of the amount of evolved gas until a plateau is reached. **1′**_TiO_2 exhibits an analogous TON vs *t* trend, just a minor decrease in the slope and a much smaller (if any) induction time are observed. In contrast, the first supernatant solution shows a sigmoidal trend (Figure 1), indicating an increase in the activity at the end of the catalytic process.

The second supernatant is not active at all (Figure 1). It can be supposed that some iridium catalytic centers, more weakly bound to the solid support in **1**_TiO_2, leach out during the first catalytic run. The content of iridium in **1′**_TiO_2 was evaluated by ICP-OES. It was found that ∼30.0% of the iridium of **1**_TiO_2 is released into the solution during the reaction with CAN, and thus, the calculated iridium loading in **1′**_TiO_2 is 2.2 μmol g^{-1}. This also allowed the concentration of iridium in the supernatant to be derived (Table 1). Consequently, the TOF of the supernatant solution, calculated in the last part of the TON vs *t* trends, where the slope is maximum, is in the 6.9−14.3 min^{-1} range (Table 1, entries 2, 8, and 15). The catalytic activity of the recovered solid drops by 13−44% after each run (Table 1), and the decrease seems to be higher when a higher concentration of CAN is used (compare entries 1, 3, 5, 6 with entries 7, 9, 11, 13 and entries 14, 16, 18 in Table 1). Suspecting that at least part of this drop could be due to some loss of catalyst during the centrifugation and, especially, washing procedures, we repeated the experiment with 62 mg of **1**_TiO_2 and 250 μmol of CAN, thus reproducing the same conditions of the experiment whose results are reported in entries 14−18 of Table 1, separating the supernatant and washing the solid only after the first catalytic run. Successive runs were performed by adding fresh aliquots of CAN, after centrifugation and removal of supernatant, without washing the powder (entries 19−23 in Table 1). Results clearly indicate a much smaller drop of activity (compare entries 14, 16, 18 with entries 19, 20, 21 in Table 1).

2.1. Catalytic Water Oxidation with 1′_TiO_2.

Having realized that the material recovered after the first catalytic run (**1′**_TiO_2) does not undergo further leaching, we decided to prepare **1′**_TiO_2 in large quantity, as described in the Experimental Section, and evaluate its catalytic performance in terms of TOF, TON, and reusability in more detail. With this as the goal, multiple aliquots of 100 μL of CAN (50 μmol) were repeatedly added to suspensions of about 56, 28, and 13 mg of **1′**_TiO_2, respectively, in 5 mL of acidic water (pH 1, 0.1 M HNO_3) (Table 2). Because the **1′**_TiO_2 material contained

Table 2. Three Experiments in Which Multiple Catalytic Aliquots of around 50 μmol of CAN (100 μL) Were Added to Different Amounts of 1′_TiO_2 Dispersed in 5 mL of Acidic Water (pH 1, 0.1 M HNO_3)

entry	run	C_{Ir} (μM)[b]	C_{CAN} (mM)	C_{CAN}/C_{Ir}	TOF[a] (min^{-1})[c]	total cycles[d]
1	I	**24.3 (25.0)**	10.0	**412**	**9.1 (5.9)**	77
2	II	23.8 (24.4)	9.9	416	7.0 (4.5)	155
3	III	23.3 (23.8)	9.7	416	5.5 (3.4)	227
4	IV	22.9 (23.3)	9.5	415	5.3 (2.4)	309
5	V	22.5 (22.7)	9.3	413	5.2 (2.2)	391
6	VI	22.1 (22.2)	9.2	416	4.1 (1.9)	456
7	VII	21.7 (21.7)	9.0	415	3.8 (1.8)	534
8	VIII	21.3 (21.3)	8.9	418	3.3 (1.7)	605
9	IX	21.0 (20.8)	8.7	414	3.0 (1.6)	675
10	X	20.6 (20.4)	8.6	417	2.8 (1.5)	746
11	I	**12.0**	10.0	**833**	**15.1**	166
12	II	11.8	9.4	797	9.2	317
13	III	11.6	9.8	819	7.5	489
14	IV	11.4	9.6	842	6.5	653
15	V	11.2	9.4	839	5.8	801
16	VI	11.0	9.0	818	5.3	954
17	VII	10.8	8.9	824	4.8	1110
18	VIII	10.6	8.7	821	4.4	1263
19	I	**5.7**	10.0	**1754**	**16.6**	333
20	II	5.6	9.8	1750	9.9	714
21	III	5.5	9.6	1745	8.1	1033
22	IV	5.4	9.5	1759	6.2	1304
23	V	5.3	9.3	1755	5.9	1644
24	VI	5.2	9.1	1750	5.4	1953

[a]TOF values in parentheses refer to a multiple run experiment carried out using **1** as homogeneous catalyst (C_{Ir} = 25 μM, C_{CAN} = 10 mM). [b]Based on a catalyst loading of 2.2 μmol g^{-1} (70.0% of the initial value based on ICP-OES data). [c]From $(k_{obs}/mol_{Ir})\cdot 60$ (where k_{obs} is derived from gas(mol) produced vs time(s) linear trend in the first part of the reaction, corrected for dilution factors). [d]Cumulative catalytic cycles performed in each run.

2.2 μmol g^{-1} of iridium catalyst (see above), in the three experiments reported in Table 2, about 420, 820, and 1800 equiv of CAN, respectively, were added in each consecutive addition.

As found before (Table 1), TOF values increase with increasing C_{CAN}/C_{Ir} ratio value (Figure 2). In particular, in the first experiment, in which C_{CAN}/C_{Ir} = 412, a TOF value of 9.1 min^{-1} was measured (Table 2, entry 1), whereas in the second and in the third experiments, in which C_{CAN}/C_{Ir} was equal to 833 and 1754, respectively, TOF values were 15.1 and 16.6 min^{-1} (Table 2, entries 11 and 19).

A drop in the activity was observed in the three experiments after each catalytic run (Table 2): TOF values decreased from 9.1 to 2.8 min^{-1} moving from the 1st to the 10th catalytic run

dx.doi.org/10.1021/cs501590k | ACS Catal. 2015, 5, 264−271

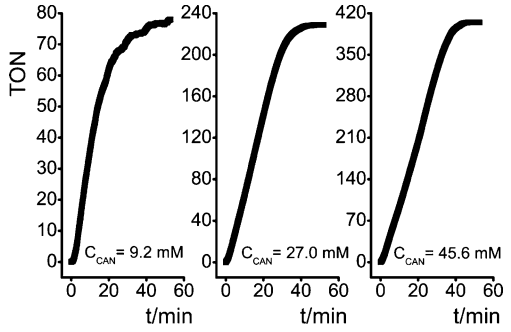

Figure 2. TON versus time trends for catalytic experiments carried out by II_{solid} (C_{Ir} = 24.5−24.6 μM, pH 1, 0.1 M HNO_3) at different concentrations of CAN (data are reported in Table 1, entries 3, 9, and 16).

with 420 equiv of CAN (Table 2, entries 1−10); over 8 catalytic runs of 820 equiv of CAN each, TOF values decreased from 15.1 to 4.4 min^{-1} (Table 2, entries 11−18 and Figure 2); and finally, in the last experiment reported in Table 2 (entries 19−24), after 6 consecutive additions of around 1800 equiv of CAN, TOF values dropped from 16.6 to 5.4 min^{-1}.

Catalyst deactivation seems to be more evident when many additions of a small amount of CAN are performed. For example, after around 700 catalytic cycles, in the first experiment reported in Table 2, the TOF value (entry 10) corresponds to 31% of the initial value (entry 1), whereas in the second experiment (entry 14) it is 43% of it (entry 11), and in the last (entry 20), it corresponds to 60% of the initial TOF value (entry 19). Notably, in this last experiment, **1**′_TiO_2 is still active with a TOF of 5.4 min^{-1} after a total of 1953 catalytic cycles (Table 2, entry 24).

A direct comparison between the catalytic activity of immobilized **1**′_TiO_2 and homogeneous **1** was performed, carrying out a multiple run experiment also for **1** under experimental conditions as similar as possible to those used for **1**′_TiO_2 (see TOF values in parentheses of entries 1−10 in Table 2 and Figure 3). TOF values for **1**′_TiO_2 decrease from 9.1 min^{-1} (run 1) to 2.8 min^{-1} (run 10). Those of **1** are almost two times lower and pass from 5.9 min^{-1} (run 1), a value perfectly consistent with what previously reported by us,[42] down to 1.5 min^{-1} (run 10) (Table 2). On the other hand, the two catalytic systems exhibit comparable TON values. It is

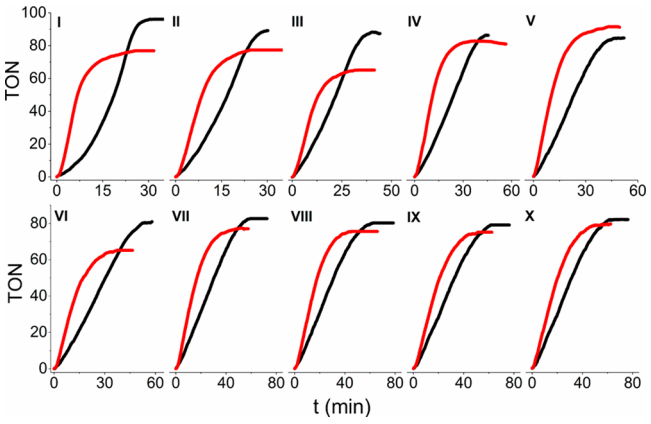

Figure 3. TON versus time trends for two multiple run experiments carried out for **1**′_TiO_2 (red) and **1** (black) under very similar experimental conditions (entries 1−10, Table 2).

interesting to note that none of the catalytic runs with **1**′_TiO_2 show any induction period, whereas some increase of activity is observed in the first 2−3 catalytic runs with **1** (Figure 3).

The pronounced decrease in the activity observed when more CAN additions were performed using the same total number of equivalents seems to indicate that **1**′_TiO_2 could exhibit better performances when a single addition of a large excess of CAN is used. This was just the case. When a single aliquot of 46915 equiv of CAN was added to a suspension of **1**′_TiO_2, a TON of 6596 was measured after ∼16 h, and notably, a constant TOF of 12.8 min^{-1} was observed for more than 6 h (>5000 catalytic cycles) (Figure S6, Supporting Information). The latter catalytic performances are outstanding.

2.2. Structural and Morphological Characterization of 1_TiO_2 and 1′_TiO_2. The PXRD patterns of **1**_TiO_2 and **1**′_TiO_2 (Figure 4) are identical, as is usually the case when

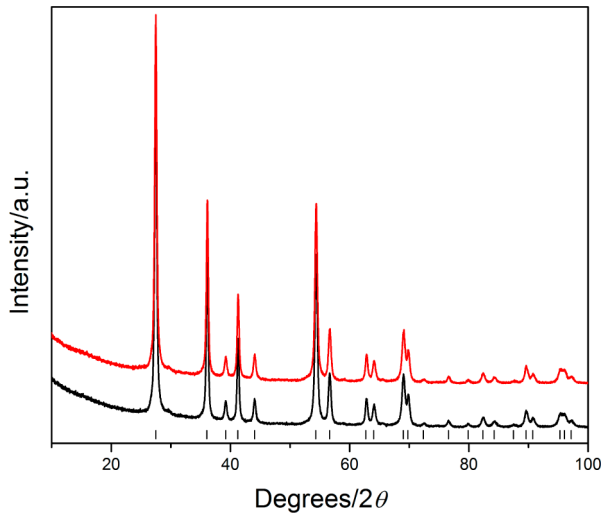

Figure 4. X-ray powder diffraction patterns of **1**_TiO_2 (black line) and **1**′_TiO_2 (red line). Black marks indicate the calculated positions of rutile peaks.

small amounts of metals are deposited on a crystalline support. They show that no other diffraction peaks except those belonging to the rutile substrate phase emerged after functionalization and after the first catalytic run. Furthermore, no additional line broadening is observed in the pattern after the catalytic run, also showing that microstructural parameters (crystallite size and lattice defects) are similar for the two samples.

These observations were confirmed by FE-SEM and TEM analysis. TEM micrographs of the pristine TiO_2 and the two samples did not show relevant differences. As an example, Figure 5 shows a TEM image of **1**′_TiO_2. All of these images show samples made of prismatic crystallites with dimensions of ∼30 nm × 100 nm (± 10 nm), and no highly contrasted structures that might be ascribed to heavy iridium phases were observed.

Elemental mappings of Ir and Cl in **1**_TiO_2 and **1**′_TiO_2 samples were obtained by the FE-SEM−EDS technique (Figure S10, Supporting Information). In these images, the local concentration of one element is indicated by the brightness and the intensity of the black spots. From these data, we can conclude that iridium atoms are uniformly distributed throughout the particles of the two samples. They also show that distribution of Cl nicely tracks that of Ir in both **1**_TiO_2

dx.doi.org/10.1021/cs501590k | ACS Catal. 2015, 5, 264−271

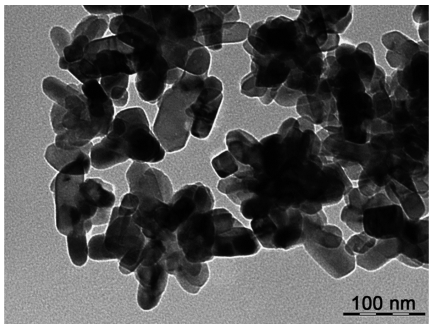

Figure 5. TEM image of **1**′_TiO_2. Scale bar corresponds to 100 nm.

and **1**′_TiO_2. The comparison between iridium and chlorine maps taken before and after a catalytic run seems to confirm, although qualitatively, the reduction of immobilized catalyst content indicated by ICP data.

In summary, combining PXRD and electron microscopy data, it is possible to state that iridium atoms are uniformly dispersed on the samples before and after the catalytic run and do not form separate aggregates larger than a few nanometers.

2.3. XPS Spectroscopy Studies. X-ray photoelectron spectroscopy was conducted on **1**_TiO_2 to extract quantitative information on the surface composition of the catalyst. The overlap between the Ti 3s and Ir $4f_{7/2}$ makes it difficult to accurately compute for the amount of Ir on the surface as well as to investigate its chemical state. However, because the Ir $4f_{5/2}$ line is above that of Ti 3s, it is possible to recalculate the amount of Ir $4f_{7/2}$ and deduct it from the overall peak seen at the Ti 3s/Ir $4f_{7/2}$ position. Figure 6 presents the Ti 3s region in

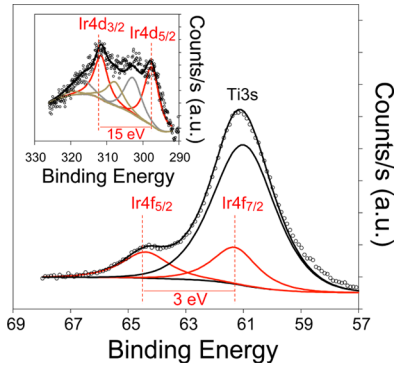

Figure 6. XPS Ti 3s/Ir 4f of **1**_TiO_2 before reaction. Inset: XPS Ir 4d region. Spin splitting is indicated by ΔE.

which a fitting for the Ir $4f_{5/2}$ at a BE of 64.4 eV was made. On the basis of the splitting between the Ir $4f_{7/2,5/2}$ of 3.0 eV,[70,71] a peak at 61.3 eV was generated with a theoretical contribution of 4/3 times that of Ir $4f_{5/2}$.

To further confirm the Ir presence, we sought the Ir 4d region; typically, 3−5 times weaker than that of Ir 4f. The inset in Figure 6 presents the Ir 4d region, which lies just above the C 1s region, making the background high, which further affects the signal-to-noise ratio. The presence of the two peaks with a splitting of 15.0 eV can be additional evidence for Ir. Therefore, we have curve-fitted for the two main peaks at 297.0 and 312.0 eV attributed to Ir $4d_{5/2}$ and Ir $4d_{3/2}$ respectively (BE position are with ±0.2 eV due to the weak signal-to-noise ratio). Other peaks above each line are, however, present by ∼5 and 9 eV. The large separation of these two peaks from the parent ones rules out possible attribution to changes in the chemical environment of the Ir atoms. These can be tentatively attributed to shake-up satellites; however, detailed satellite structures of Ir 4d are not available to enforce their attributions. To further probe into the Ir signal, we have chosen to sputter of Ar ions on the surface. Ion sputtering does affect the surface in several ways in addition to cleaning it from adventitious contaminants. It reduces the heavy elements due to preferential removal of oxygen atoms (leaving behind electrons).[72] In the process, however, some Ir may have been sputtered away, too, as a result of breaking the Ir−O and Ir−N bonds. The Supporting Information presents the Ir 4d region upon Ar ions sputtering. Although the signal-to-noise has further decreased because of the rise of the baseline due to some Ar ions that are implanted on the surface (Ar 2s lines are at ∼319.5 eV), the Ir signal still persists, albeit slightly smaller.

In summary, the presence of Ir $4f_{5/2}$, and Ir 4d in the fresh sample and the persistence of the signal of the Ir 4d in the sputtered surface give confidence that, indeed, Ir complexes have been deposited on the surface of TiO_2 and are responsible for the enhancement of the oxygen evolution reaction. Table 3 gives the computed peak areas. On the basis of the 4f lines, Ir represents ∼0.6 at. % of the surface (neglecting satellite contributions) with an Ir/Ti ratio of ∼0.02.

Table 3. Quantitative Analysis of 1_TiO_2 Using XPS Based on Both the Ir 4d and Ir 4f

	Ir/Ti atomic	Ir at. %
based on Ir 4d (with satellites)	0.037	1.10
based on Ir 4d (without satellites)	0.020	0.70
based on Ir 4f	0.018	0.60

3. CONCLUSIONS

We demonstrated that the immobilization of a molecular catalyst onto the surface of a properly selected functional material is a very promising strategy to develop efficient catalysts for water oxidation. As a matter of fact, the previously reported molecular catalyst [Ir(HEDTA)Cl]Na (**1**)[42] improves its performance toward water oxidation when immobilized onto rutile TiO_2. All techniques exploited to characterize the immobilized catalyst, both before (**1**_TiO_2) and after (**1**′_TiO_2) the first catalytic run, indicated that iridium is uniformly dispersed on the samples, thus excluding the formation of domains of aggregation, at least with nanometric dimensions.

The results reported in this paper are extremely encouraging for future applications of this material and analogous ones in photocatalytic water oxidation. Experiments in such a direction are in progress in our laboratories.

4. EXPERIMENTAL SECTION

Complex **1** was synthesized by the reaction of $IrCl_3.nH_2O$ with Na_2H_2EDTA according to a literature procedure.[73]

Preparation of 1_TiO_2. A solution of complex **1** (3.9−7.7 mg) in Milli-Q water (∼2 mL) was added to rutile TiO_2 nanoparticles (0.8−1.7 g) dispersed in water (∼5 mL) at 25 °C. The mixture was kept under stirring for a few hours, and afterward, the solid was recovered by centrifugation; the latter was washed several times with water, 0.1 M of HNO_3, acetonitrile, dichloromethane and, finally, dried under vacuum.

dx.doi.org/10.1021/cs501590k | ACS Catal. 2015, 5, 264−271

Preparation of 1′_TiO_2. A 300 mg portion of **1**_TiO_2 was reacted with 0.242 mmol of CAN in a total volume of 5.5 mL of water at pH 1 (by HNO_3) at 25 °C. The water oxidation reaction was monitored by manometry (see below), and when the gas production was finished, the mixture was centrifuged. The supernatant solution was collected for elemental analysis, and the solid was recovered and washed two times with a 0.1 M solution of HNO_3 in water and three times with Milli-Q water. Finally, the solvent was removed by evaporation under reduced pressure and the solid **1**′_TiO_2 was dried under vacuum.

Water Oxidation Experiments. Water oxidation experiments were performed at pH 1 (by HNO_3) using CAN as the sacrificial oxidant. Gas production was monitored through manometric measurements performed with homemade water-jacket glass tubes coupled to a Testo 521-1 manometer.

In a first series of experiments, a **1**_TiO_2 sample (62.1−62.4 mg) was transferred in a homemade glass tube (working cell) equipped with a side arm for the connection with the manometer and with a septum for the injection of the oxidant solution. A stir bar was placed inside the tube, and 5 mL of water at pH 1 (by HNO_3) was added to the solid. The same amount of solvent was transferred into another identical glass tube (reference cell). Both tubes were closed with a septum and connected to the manometer. The system was kept at a constant temperature of 25 °C and allowed to equilibrate with stirring for at least 20 min. When a steady baseline was achieved, the solvent solution (0.5 mL) was added into the reference cell, and the oxidant solution (0.5 mL, 0.051−0.251 mmol) was added into the working cell. Gas evolution was monitored during the reaction by measuring the differential pressure between the two cells.

Once the gas production was finished (because the sacrificial oxidant was all consumed), the mixture into the working cell was centrifuged. Supernatant solution (4.5−4.7 mL) was recovered and tested in water oxidation by the addition of the same amount of CAN used for the previous reaction. The remaining solid was washed two times with acidic water (pH 1, 0.1 M HNO_3) and reused for several catalytic runs performed under exactly the same conditions. After each catalytic run, the solid was centrifuged and washed 2−3 times with acidic water. In some cases, the activity of the recovered supernatant solutions was tested.

The rate constant k_{obs} (mol s^{-1}) was derived from gas evolution (mol)-vs-time (s) linear trends in the first part of the reaction. The k_{obs} values derived for the experiments carried out with supernatant solutions were corrected for dilution factors to better compare their values with the ones observed in the reaction with the solid. Entries 19−23 of Table 1 refer to an experiment in which the solid was washed only after the first catalytic run and reused in subsequent catalytic runs after centrifugation, removal of the supernatant, and addition of fresh acidic solution. TOF (min^{-1}) values were calculated from (k_{obs}/mol_{Ir})·60, where mol_{Ir} is the amount of iridium contained in the solid material or in supernatant solutions used in the reactions, based on ICP-OES data. All results obtained in these experiments are summarized in Table 1.

In another series of experiments, a **1**′_TiO_2 sample (13.245−56.245 mg) was transferred into the working cell, and 5.0 mL of acidic water (pH 1, 0.1 M HNO_3) was added to the solid. The same amount of solvent was transferred into the reference cell, and both tubes were kept at a constant temperature of 25 °C and connected to the manometer and were allowed to equilibrate with stirring for at least 20 min. When a steady baseline was achieved, the solvent solution (100 μL) was added into the reference cell, and the oxidant solution (100 μL, 0.051−0.052 mmol) was added into the working cell. Gas evolution was monitored by manometry, and once the gas production stopped, both tubes were disconnected from the manometer. The system was allowed to re-equilibrate at atmospheric pressure, and then it was reconnected to the manometer for another catalytic run that was carried out as the previous one. This procedure was repeated 6−10 times. The k_{obs} values were derived from gas evolution (mol)-vs-time (s) linear trends in the first part of the reaction and corrected for dilution factors. TOF (min^{-1}) values were calculated from (k_{obs}/mol_{Ir})·60, where mol_{Ir} is the amount of iridium contained in the solid material used in the reactions, based on ICP-OES data. All results obtained in these experiments are collected in Table 2.

Finally, the maximum number of catalytic cycles (TON) that catalyst **1**′_TiO_2 can undergo was determined in a manometric experiment in which 1.45 mL of the oxidant solution (1.092 mmol) was added to a suspension of 10.580 mg of **1**′_TiO_2 in 0.5 mL of acidic water (pH 1, 0.1 M HNO_3) (see the Supporting Information).

A maximum a priori error of ∼20% in TON and TOF was estimated by considering the uncertainty of weighting, preparation of catalyst and CAN solutions, CAN injection, instrumental precision, standard deviation of TON-vs-*t* trends (only for TOF).

Instrumental Measurements. PXRD patterns were taken with a Philips X'PERT PRO MPD diffractometer operating at 40 kV and 40 mA with a step size 0.017° 2θ and step scan 150 s using Cu Kα radiation and an X'Celerator fast detector.

The morphology of the samples was investigated with a Philips 208 transmission electron microscope and with a FEG LEO 1525, scanning electron microscope. This latter instrument supported an energy dispersive X-ray spectrometer for elemental Ir mapping.

FE-SEM micrographs were collected after depositing the samples on a stub and sputter-coating with chromium for 20 s.

Metal analysis was performed with Varian 700-ES series inductively coupled plasma-optical emission spectrometers. A concentrated stock solution of iridium was prepared by dissolving dried $IrCl_3$ in concentrated HCl until reaching a volume of 1 L of solution. Working calibration solutions were prepared from the stock solution by making 300-, 100-, 60-, and 30-fold dilutions.

For the analysis of **1**_TiO_2, a weighed amount of the solid (∼180 mg) and ∼500 mg of $(NH_4)_2SO_4$ were dissolved in ∼40 mL of H_2SO_4 under reflux at T ∼ 350 °C. The solution was allowed to cool to room temperature and then brought to a final volume of 50 mL by the addition of Milli-Q water. A diluted solution (1:2) was used for ICP analysis, and the iridium content was determined by ICP-OES.

The supernatant solution collected after a catalytic run during the procedure followed for the preparation of **1**′_TiO_2 (see text above) was directly analyzed by ICP-OES for determining the amount of iridium released during catalysis.

X-ray photoelectron spectroscopy was conducted using a Thermoscientific ESCALAB 250 Xi equipped with a monochromated Al Kα X-ray source, UV He lamp for UPS, ion scattering spectroscopy, and reflected electron energy loss spectroscopy was used. The base pressure of the chamber was typically in the low 10^{-10} mbar range. Charge neutralization was used for all samples (compensating shifts of ∼1 eV). Spectra

dx.doi.org/10.1021/cs501590k | ACS Catal. 2015, 5, 264−271

were calibrated with respect to C 1s at 284.7 eV. The Ti 3s/Ir 4f, Ti 2p, O 1s, and Ir 4d were scanned for both the fresh and used catalysts. Typical acquisition conditions were as follows: pass energy = 20 eV and scan rate = 0.1 eV per 200 ms. Ar ion bombardment was performed with an EX06 ion gun at 1 kV beam energy and 10 mA emission current; sample current was typically 0.9−1.0 μA. The sputtered area of 900 × 900 μm^2 was larger than the analyzed area: 600 × 600 μm^2. Self-supported oxide disks of ∼0.5 cm diameter were loaded into the chamber for analysis. Data acquisition and treatment was done using Avantage software.

■ ASSOCIATED CONTENT

Supporting Information

The following file is available free of charge on the ACS Publications website at DOI: 10.1021/cs501590k.

Additional figures on catalytic experiments and analytical characterization of immobilized catalysts (PDF)

■ AUTHOR INFORMATION

Corresponding Author

*Phone +39 075 5855579. Fax +39 075 5855598. E-mail: alceo.macchioni@unipg.it.

Notes

The authors declare no competing financial interest.

■ ACKNOWLEDGMENTS

We thank SABIC and Regione Umbria (POR FSE Projects) for financial support.

■ REFERENCES

(1) Lewis, N. S.; Nocera, D. G. *Proc. Natl. Acad. Sci. U.S.A.* **2006**, *103*, 15729−15735.
(2) Balzani, V.; Credi, A.; Venturi, M. *ChemSusChem* **2008**, *1*, 26−58.
(3) Gust, D.; Moore, T. A.; Moore, A. L. *Acc. Chem. Res.* **2009**, *42* (12), 1890−1898.
(4) Alstrum-Acevedo, J. H.; Brennaman, M. K.; Meyer, T. J. *Inorg. Chem.* **2005**, *44*, 6802−6827.
(5) Dau, H.; Limberg, C.; Reier, T.; Risch, M.; Roggan, S.; Strasser, P. *ChemCatChem.* **2010**, *2*, 724−761.
(6) Inoue, H.; Shimada, T.; Kou, Y.; Nabetani, Y.; Masui, D.; Takagi, S.; Tachibana, H. *ChemSusChem* **2011**, *4*, 173−179.
(7) Lichterman, M. F.; Carim, A. I.; McDowell, M. T.; Hu, S.; Gray, H. B.; Brunschwig, B. S.; Lewis, N. S. *Energy Environ. Sci.* **2014**, *7*, 3334−3337.
(8) Wiechen, M.; Najafpour, M. M.; Allakhverdiev, S. I.; Spiccia, L. *Energy Environ. Sci.* **2014**, *7*, 2203−2212.
(9) Ahn, H. S.; Yano, J.; Don Tilley, T. *Energy Environ. Sci.* **2013**, *6*, 3080−3087.
(10) Deng, X.; Tüysüz, H. *ACS Catal.* **2014**, *4*, 3701−3714.
(11) Ruettinger, W.; Dismukes, G. C. *Chem. Rev.* **1997**, *97*, 1−24.
(12) Yagi, M.; Kaneko, M. *Chem. Rev.* **2001**, *101*, 21−36.
(13) Limburg, B.; Bouwman, E.; Bonnet, S. *Coord. Chem. Rev.* **2012**, *256*, 1451−1467.
(14) Hetterscheid, D. G. H.; Reek, J. N. H. *Angew. Chem., Int. Ed.* **2012**, *51*, 9740−9747.
(15) Jiao, F.; Frei, H. *Energy Environ. Sci.* **2010**, *3*, 1018−1027.
(16) Hansen, R. E.; Das, S. *Energy Environ. Sci.* **2014**, *7*, 317−322.
(17) Song, F.; Ding, Y.; Ma, B.; Wang, C.; Wang, Q.; Du, X.; Fu, S.; Song, J. *Energy Environ. Sci.* **2013**, *6*, 1170−1184.
(18) Leung, C.-F.; Ng, S.-M.; Ko, C.-C.; Man, W.-L.; W.-L. Wu, W.-L.; Chen, L.; Lau, T.-C. *Energy Environ. Sci.* **2012**, *5*, 7903−7907.
(19) Yagi, M.; Syouji, A.; Yamada, S.; Komi, M.; Yamazak, H.; Tajima, S. *Photochem. Photobiol. Sci.* **2009**, *8*, 139−147.
(20) Wasylenko, D. J.; Palmer, R. D.; Berlinguette, C. P. *Chem. Commun.* **2013**, *49*, 218−227.
(21) Cao, R.; Lai, W.; Du, P. *Energy Environ. Sci.* **2012**, *5*, 8134−8157.
(22) Liu, X.; Wang, F. *Coord. Chem. Rev.* **2012**, *256*, 1115−1136.
(23) For a comparison between homogeneous and heterogeneous water oxidation catalysts see: Fukuzumi, S.; Hong, D. *Eur. J. Inorg. Chem.* **2014**, 645−659. Vickers, J. W.; Lv, H.; Sumliner, J. M.; Zhu, G.; Luo, Z.; Musaev, D. G.; Geletii, Y. V.; Hill, C. L. *J. Am. Chem. Soc.* **2013**, *135*, 14110−14118. Stracke, J. J.; Finke, R. G. *ACS Catal.* **2014**, *4*, 909−933.
(24) (a) Grotjahn, D. B.; Brown, D. B.; Martin, J. K.; Marelius, D. C.; Abadjian, M.-C.; Tran, H. N.; Kalyuzhny, G.; Vecchio, K. S.; Specht, Z. G.; Cortes-Llamas, S. A.; Miranda-Soto, V.; van Niekerk, C.; Moore, C. E.; Rheingold, A. L. *J. Am. Chem. Soc.* **2011**, *133*, 19024−19027. (b) Zuccaccia, C.; Bellachioma, G.; Bolaño, S.; Rocchigiani, L.; Savini, A.; Macchioni, A. *Eur. J. Inorg. Chem.* **2012**, 1462−1468. (c) Wang, C.; Wang, J.-L.; Lin, W. *J. Am. Chem. Soc.* **2012**, *134*, 19895−19908. (d) Zuccaccia, C.; Bellachioma, G.; Bortolini, O.; Bucci, A.; Savini, A.; Macchioni, A. *Chem.- Eur. J.* **2014**, *20*, 3446−3456. (e) Zhang, T.; de Krafft, K. E.; Wang, J.-L.; Wang, C.; Lin, W. *Eur. J. Inorg. Chem.* **2014**, *4*, 698−707.
(25) Young, K. J.; Martini, L. A.; Milot, R. L.; Snoeberger, R. C., III; Batista, V. S.; Schmuttenmaer, C. A.; Crabtree, R. H.; Brudvig, G. W. *Coord. Chem. Rev.* **2012**, *256*, 2503−2520.
(26) Berardi, S.; La Ganga, G.; Puntoriero, F.; Sartorel, A.; Campagna, S.; Bonchio, M. *Photochemistry* **2012**, *40*, 274−294.
(27) Brimblecombe, R.; Dismukes, G. C.; Swiegers, G. F.; Spiccia, L. *Dalton Trans.* **2009**, 9374−9384.
(28) Duan, L.; Tong, L.; Xu, Y.; Sun, L. *Energy Environ. Sci.* **2011**, *4*, 3296−3313.
(29) Moore, G. F.; Blakemore, J. D.; Milot, R. L.; Hull, J. F.; Song, H.-E.; Cai, L.; Schmuttenmaer, C. A.; Crabtree, R. H.; Brudvig, G. W. *Energy Environ. Sci.* **2011**, *4*, 2389−2392.
(30) Lin, L.; Duan, L.; Xu, Y.; Gorlov, M.; Hagfeldt, A.; Sun, L. *Chem. Commun.* **2010**, *46*, 7307−7309.
(31) Honda, K.; Fujishima, A. *Nature* **1972**, *238*, 37−38.
(32) Grätzel, M. *Nature* **2001**, *414*, 338−344.
(33) Waterhouse, G. I. N.; Wahab, A. K.; Al-Oufi, M.; Jovic, V.; Sun-Waterhouse, D.; Dalaver, A.; Llorca, J.; Idriss, H. *Sci. Rep.* **2013**, *3* (2849), 1−5.
(34) Connelly, K. A.; Idriss, H. *Green Chem.* **2012**, *14*, 260−280.
(35) Liu, F.; Cardolaccia, T.; Hornstein, B. J.; Schoonover, J. R.; Meyer, T. J. *J. Am. Chem. Soc.* **2007**, *129*, 2446−2447.
(36) Chen, Z.; Conception, J. J.; Jurss, J. W.; Meyer, T. J. *J. Am. Chem. Soc.* **2009**, *131*, 15580−15581.
(37) Francàs, L.; Sala, X.; Benet-Buchholz, J.; Escriche, L.; Llobet, A. *ChemSusChem* **2009**, *2*, 321−329.
(38) McDaniel, N. D.; Coughlin, F. J.; Tinker, L. L.; Bernhard, S. *J. Am. Chem. Soc.* **2008**, *130*, 210−217.
(39) Hull, J. F.; Balcells, D.; Blakemore, J. D.; Incarvito, C. D.; Eisenstein, O.; Brudvig, G. W.; Crebtree, R. H. *J. Am. Chem. Soc.* **2009**, *131*, 8730−8731.
(40) Savini, A.; Bellachioma, G.; Ciancaleoni, G.; Zuccaccia, C.; Zuccaccia, D.; Macchioni, A. *Chem. Commun.* **2010**, *46*, 9218−9219.
(41) Savini, A.; Belanzoni, P.; Bellachioma, G.; Zuccaccia, C.; Zuccaccia, D.; Macchioni, A. *Green Chem.* **2011**, *13*, 3360−3374.
(42) Savini, A.; Bellachioma, G.; Bolaño, S.; Rocchigiani, L.; Zuccaccia, C.; Zuccaccia, C.; Zuccaccia, D.; Macchioni, A. *ChemSusChem* **2012**, *5*, 1415−1419.
(43) Bucci, A.; Savini, A.; Rocchigiani, L.; Zuccaccia, C.; Rizzato, S.; Albinati, A.; Llobet, A.; Macchioni, A. *Organometallics* **2012**, *31*, 8071−8074.
(44) Savini, A.; Bucci, A.; Bellachioma, G.; Giancola, S.; Palomba, F.; Rocchigiani, L.; Rossi, A.; Suriani, M.; Zuccaccia, C.; Macchioni, A. *J. Organomet. Chem.* **2014**, *771*, 24−32.
(45) Blakemore, J. D.; Schley, N. D.; Balcells, D.; Hull, J. F.; Olack, G. W.; Incarvito, C.; Eisenstein, O.; Brudvig, G. W.; Crebtree, R. H. *J. Am. Chem. Soc.* **2010**, *132*, 16017−16029.

(46) Lalrempuia, R.; McDaniel, N. D.; Mueller-Bunz, H.; Bernhard, S.; Albrecht, M. *Angew. Chem., Int. Ed.* **2010**, *49*, 9765−9768.
(47) Hetterscheid, D. G. H.; Reek, J. N. H. *Chem. Commun.* **2011**, *47*, 2712−2714.
(48) Dzik, W. I.; Calvo, S. E.; Reek, J. N. H.; Lutz, M.; Ciriano, M. A.; Tejel, C.; Hetterscheid, D. G. H.; de Bruin, B. *Organometallics* **2011**, *30*, 372−374.
(49) Marquet, N.; Gärtner, F.; Losse, S.; Pohl, M.-M.; Junge, H.; Beller, M. *ChemSusChem* **2011**, *4*, 1598−1600.
(50) Petronilho, A.; Rahman, M.; Woods, J. A.; Al-Sayyed, H.; Muller-Bunz, H.; Don, M. J. M.; Bernhard, S.; Albrecht, M. *Dalton Trans.* **2012**, *41*, 13074−13080.
(51) Codalà, Z.; Cardoso, J. M. S.; Royo, B.; Costa, M.; Fillol, J. L. *Chem. - Eur. J.* **2013**, *19*, 7203−7213.
(52) Petronilho, A.; Woods, J. A.; Bernhard, S.; Albrecht, M. *Eur. J. Inorg. Chem.* **2014**, *4*, 708−714.
(53) Hong, D.; Murakami, M.; Yamada, Y.; Fukuzumi, S. *Energy Environ. Sci.* **2012**, *5*, 5708−5716.
(54) Woods, J. A.; Lalrempuia, R.; Petronilho, A.; McDaniel, N. D.; Müller-Bunz, H.; Albrecht, M.; Bernhard, S. *Energy Environ. Sci.* **2014**, *7*, 2316−2328.
(55) Guo, Q.; Cocks, I.; Williams, E. M. *Surf. Sci.* **1997**, *393*, 1−11.
(56) Guo, Q.; Williams, E. M. *Surf. Sci.* **1999**, *433*−*435*, 322−326.
(57) Qiu, T.; Barteau, M. A. *J. Colloid Interface Sci.* **2006**, *303*, 229−235.
(58) Cocks, D.; Guo, Q.; Williams, E. M. *Surf. Sci.* **1997**, *390*, 119−125.
(59) Mattsson, A.; Hu, S.; Hermansson, K.; Österlund, L. *J. Chem. Phys.* **2014**, *140*, 034705.
(60) Gutiérrez-Sosa, A.; Martinéz-Escolano, P.; Raza, H.; Lindsay, R.; Wincott, P. L.; Thornton, G. *Surf. Sci.* **2001**, *471*, 163−169.
(61) Sayago, D. I.; Polcik, M.; Lindsay, R.; Toomes, R. L.; Hoeft, J. T.; Kittel, M.; Woodruff, D. P. *J. Phys. Chem. B* **2004**, *108*, 14316−14323.
(62) Lerotholi, T. J.; Kröger, E. A.; Knight, M. J.; Unterberger, W.; Hogan, K.; Jackson, D. C.; Lamont, C. L. A.; Woodruff, D. P. *Surf. Sci.* **2009**, *603*, 2305−2311.
(63) Muir, J. M. R.; Costa, D.; Idriss, H. *Surf. Sci.* **2014**, *624*, 8−14.
(64) Muir, J.; Idriss, H. *Surf. Sci.* **2013**, *617*, 60−67.
(65) Muir, J.; Idriss, H. *Surf. Sci.* **2013**, *607*, 187−196.
(66) A control experiment using TiO_2 instead of **1**_TiO_2 led to negligible production of oxygen (Figure S1). Such a blank experiment was performed in ambient light waiting one hour before adding CAN. No gas was evolved. Consequently, all experiments were performed in ambient light.
(67) Apparent O_2 yield is less than 100% (Table 1) likely due to some oxygen dissolved in water that is not correctly taken into account by manometric measurements.
(68) Savini, A.; Bucci, A.; Bellachioma, G.; Rocchigiani, L.; Zuccaccia, C.; Llobet, A.; Macchioni, A. *Eur. J. Inorg. Chem.* **2014**, *4*, 690−697.
(69) Bozoglian, F.; Romain, S.; Ertem, M. Z.; Todorova, T. K.; Sens, C.; Mola, J.; Rodríguez, M.; Romero, I.; Benet-Buchholz, J.; Fontrodona, X.; Cramer, C. J.; Gagliardi, L.; Llobet, A. *J. Am. Chem. Soc.* **2009**, *131*, 15176−15187.
(70) Kono, S.; Shiraishi, M.; Plusnin, N. I.; Goto, T.; Ikejima, Y.; Abukawa, T.; Shimomura, M.; Dai, Z.; Bednarski-Meinke, C.; Goldi, B. *Diam. Relat. Mater.* **2007**, *16*, 594−599.
(71) Crotti, C.; Farnetti, E.; Filipuzzi, S.; Stener, M.; Zangrando, E.; Moras, P. *Dalton Trans.* **2007**, 133−142.
(72) Idriss, H.; Barteau, M. A. *Adv. Catal.* **2000**, *45*, 261−331.
(73) Saito, M.; Uehiro, T.; Yoshino, Y. *Bull. Chem. Soc. Jpn.* **1980**, *53*, 3531−3536.